AN ABSTRACT OF THE THESIS OF

Lisa Nalani Freeman for the degree of Master of Science in Mechanical Engineering presented on May 6, 1992. Title: A Visual Study of Hydrodynamics in a Two-Dimensional Gas-Solid Fluidized Bed

Abstract approved: Redacted for Privacy

Hydrodynamic effects play important roles in fluidized bed combustion processes. Since the motion of "bubbles" is an important influence on fluidized bed heat transfer, a better understanding of their behavior is necessary for improving the design of fluidized bed boilers.

Using a two-dimensional bed, silica sand particles were fluidized with air at room conditions. The bubbling bed was videotaped, and both qualitative and quantitative information were gathered. Bubble characteristics such as size, rise velocity and frequency were studied while particle size and superficial gas velocity were varied. Results were compared with some existing theories and other similar research. The effect of internal surfaces at several heights in the bed was also studied.

General bubble behavior agreed well with descriptions from previous

research, and the expected spherical-cap bubble shape was observed. Both bubble size and rise velocity increased with particle size and with fluid velocity. Bubble frequency increased with fluid velocity, but decreased with increasing particle size and height in the bed. These results agree with previous work done using optical probes to measure bubble characteristics. Comparisons of data with empirical models showed general agreement. The presence of internal surfaces had the effect of reducing the bubble size, rise velocity, and frequency, and also of reducing the influence of changing particle size and superficial velocity on the bed behavior.

A Visual Study of Hydrodynamics in a Two-Dimensional Gas-Solid Fluidized Bed

by

Lisa Nalani Freeman

A THESIS

submitted to

Oregon State University

in partial fulfillment of
the requirements for the
degree of

Master of Science

Completed May 6, 1992

Commencement June 1992

APPROVED:

Redacted for Privacy

Professor of Mechanical Engineering in charge of major

Redacted for Privacy

Head of Department of Mechanical Engineering

Redacted for Privacy

Dean of Graduate School

Date thesis is presented May 6, 1992

Typed by Lisa N. Freeman for Lisa N. Freeman

Table of Contents

List of Figures

Nomenclature

V_b	Bubble volume
V_w	Wake volume
θ_w	Wake angle
U_b	Bubble rise velocity
g	Gravitational constant
k	Proportionality constant
d_b	Bubble diameter
h	Distance above the distributor
h_o	Distance below the distributor where a bubble with diameter zero would be located, a constant of integration
U_o	Superficial fluid velocity
U_{mf}	Minimum fluidization velocity
L	Distance between centers of internal surfaces
d	Diameter of internal surfaces
ρ_s	Density of particles
ρ_g	Density of fluidizing gas
ΔP	Pressure drop across bed

A Visual Study of Hydrodynamics in a Two-Dimensional Gas-Solid Fluidized Bed

Introduction

Fluidized Beds and Their Properties

This thesis concerns the hydrodynamic behavior of fluidized beds. In order to understand the significance of a fluidized bed, we must first look at what it is and how it differs from other devices. Generally, a bed consists of particles with fluid such as air flowing through them. The particles are contained and supported by a distributor which also delivers the air uniformly to the bed. The behavior of the bed depends on such characteristics as its configuration, the type of fluid used, particle size and shape, particle materials, and the flow rate of the fluid.

When the flow rate of the fluid is low, the particles are undisturbed and constitute a fixed bed. The drag force on the particles remains less than their weight, and the fluid passively flows through the interstitial gaps. Some heat transfer can occur, but the particles do not move, and thus act like a porous medium. Pressure drop across the bed increases linearly with flow rate.

When the fluid velocity is increased, the drag force becomes significant, and the fixed bed becomes fluidized. With the air flowing

upward the drag force on the particles becomes equal to their weight, and the particles are levitated. The spacing between the particles becomes more regular as they adjust to make room for the increased flow. At the point where the two forces are equal, the bed is said to be incipiently fluidized, or at minimum fluidization.

At fluid velocities at and above minimum fluidization, the bed is said to be fluidized. Once the irregularities of the initial packing are overcome, the pressure drop no longer increases with flow rate (see Figure 1, Kunii and Levenspiel, 1991, p. 71). In liquid-solid beds and beds with fine particles, the spacing between the particles grows uniformly with increased flow. This is known as a *particulately* fluidized bed, or smooth fluidization.

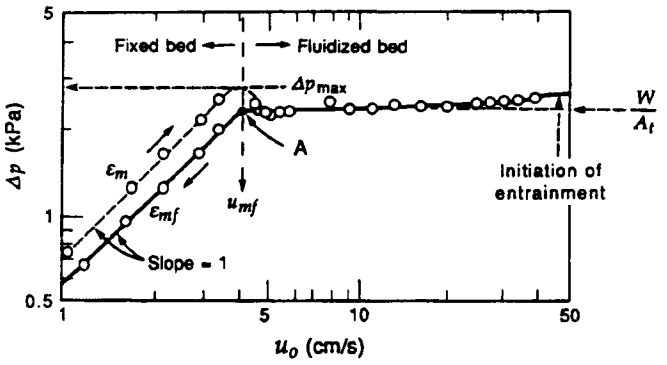

Figure 1: Pressure drop across bed.

For most gas-solid beds, particularly with relatively large particles, once the flow rate is increased beyond minimum fluidization, instabilities develop, and a phenomenon known as bubbling occurs. This is known as *aggregative* fluidization. The large voids that form within the bed resemble ordinary bubbles such as those that form in boiling water. However, these

voids are not actually bubbles since there is no interface, and air is free to flow through them. Bubble motion causes increased mixing and gross circulation in the bed which has the potential for greatly improved overall heat transfer.

At higher velocities, other forms of fluidization can occur. As fluidization becomes turbulent, violent mixing occurs, and the upper surface of the bed is ill-defined. If the particles are large or dense, or the bed is shallow, *spouting* can occur. In a spouted bed, most of the fluid flows through one channel, while much of the bed remains unfluidized. Finally, when the fluid velocity reaches the transport velocity of the particles they are carried away by the fluid (see Figure 2, Kunii and Levenspiel, 1991, p. 2).

Once a bed of particles is fluidized, it exhibits properties that are liquid-like. For example, the upper surface of the particles remains level if the bed is tipped to one side. Light objects float; solids pour out of a hole

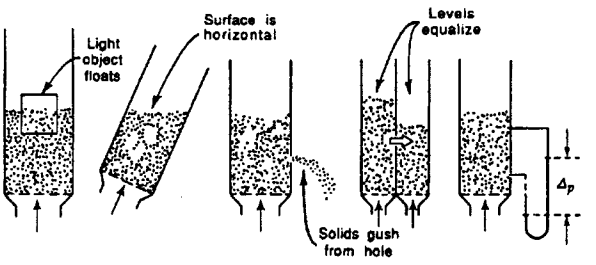

Figure 3: Liquid-like behavior of a fluidized bed.

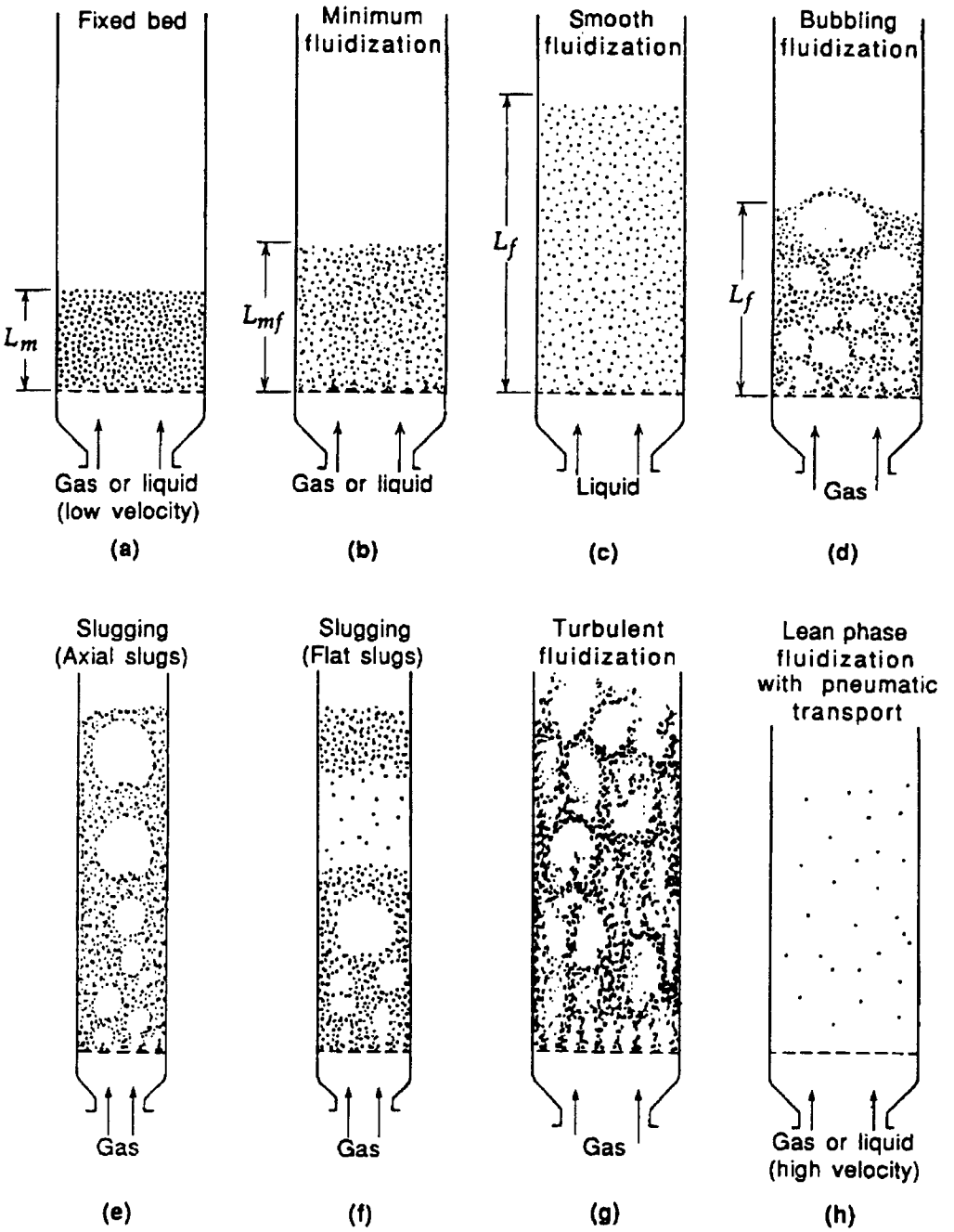

Figure 2: Fluidization regimes.

the side of the container (see Figure 3, Kunii and Levenspiel, 1991, p. 4).

Significance of Research

The use of fluidized beds for heat transfer applications is advantageous for several reasons. First, the fluid and particles have a large contact surface, which improves heat transfer and other transport processes. The intensity of mixing that occurs allows low internal temperature gradients, which is desirable for many chemical processes. Heat transfer to internal surfaces is also improved by the mixing and large contact area. The bed behaves like a fluid, which allows for continuous operation in industrial processes. The thermal inertia of the system resists rapid changes in operating conditions.

Fluidized beds have limitations which make their use unsuitable in certain situations. Much power is required to fluidize particles, especially large particles or deep beds. Because of particle motion, there is much wear inside the bed, and internal surfaces can be seriously eroded. Operating conditions vary a great deal with particle size and distribution, and flow is limited to the range which fluidizes particles in certain regimes. Bubbles are difficult to design for since they are not well understood, and yet they greatly affect heat transfer rates. Fluidized beds may not be suitable for some processes, since particles may have non-uniform residence times in the bed. Sticky particles tend to agglomerate and thus are difficult to fluidize.

Combustion of coal is an important application of fluidized beds. Coal particles are injected into beds composed of fluidized limestone particles and burned. Heat exchanger tubes located in the bed and walls receive the heat and help to maintain a relatively low operating temperature. Since high fluid velocity is required for complete combustion of the coal, large particles are used. As the coal burns, some fines are inevitably transported from the bed, and are then either returned to the bed or burned in separate cells.

Fluidized bed combustion has several distinct advantages over other combustion techniques. Low grades of coal with high sulfur content can be burned. The low combustion temperature, of approximately 850 degrees Celsius, allows calcium oxide and manganese oxide to most effectively adsorb the sulfur from the burning coal, which reduces emission of sulfur oxides. Nitrous-oxides emission is also reduced when the coal is burned at these lower temperatures.

The amount of heat transferred to internal boiler tubes is greatly affected by the behavior of bubbles in the fluidized bed. Not only do the operating conditions and particles affect bubble hydrodynamics, but the tubes also have some effect on the bubbles. Thus, it is important to study bed operation with the internals and bubbles together. Since bubbles have a significant effect on performance, more information about bubble behavior is needed in order to design a more efficient fluidized bed boiler.

Hydrodynamics

Bubble hydrodynamics is an important aspect of fluidized bed behavior that is not fully understood. Bubble shape, size, and rise velocity are known to be affected by superficial fluid velocity, particle size and size distribution, and height within the bed. An evaluation of these bubble characteristics will enable a better understanding of fluidized bed behavior.

General Description. The following qualitative discussion is based upon visual observation of fluidized-bed operation in this study, as well as a member of descriptions in the technical literature. When gas flows into the bed, bubbles form at the distributor plate and rapidly coalesce into larger bubbles. When larger particles are fluidized, long, thin cavities form in a spanwise orientation above the distributor from the streams of small coalescing bubbles. These thin lateral cavities rise intact until some instability develops, and then more common bubble shapes are formed.

Bubble Shape. Generally, bubbles have a characteristic spherical-cap shape (see Figure 4, Geldart, 1986, p. 56). The top of the bubble has a fairly smooth, round appearance, while the

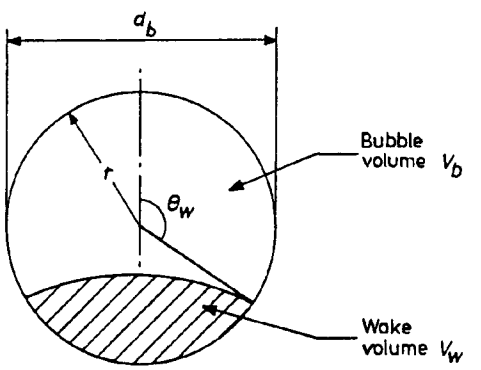

Figure 4: Model of a spherical-cap shaped bubble.

shape of the bottom of the bubble is governed by the wake. Two parameters, wake angle and wake fraction, relate the size of the wake to the related equivalent sphere which encompasses the bubble. These approximations form a bubble shape model. Actual bubble shape may deviate from this model, especially when the bubble is interacting either with other bubbles or with internals.

Bubble Size. Bubbles grow as they rise though the bed. Bubbles can increase in size by absorbing neighboring bubbles or gas flow. When a bubble gets close enough to the wake region of another bubble, it can be pulled in forming one large bubble. Two bubbles which get close enough to interact with each other will combine into a single bubble. This is called coalescence.

Bubble size can also be regulated by splitting. As a bubble grows, its rise velocity increases. When the drag on the bubble gets sufficiently large, a downward cusp develops in the roof of the bubble. This cusp grows rapidly and causes the bubble to split vertically. The smaller bubble can be reabsorbed, or two distinct bubbles may be produced. This mechanism may help to regulate bubble size.

Although bubble size is influenced by several factors, there appears to be a range of stable bubble sizes. Bubble size does increases with distance above the distributor and with excess gas velocity (Kunii and Levenspiel, 1991, p. 127). However, there is a maximum stable bubble size (Kunii and

Levenspiel, 1991, pp. 130, 146), although it may be too great to measure in beds of large particles. A minimum stable bubble size may also occur; several researchers have noticed that bubbles smaller than a critical size shrink and disappear (Botterill, 1975, p. 22). This critical size may also vary with height above the distributor.

Particle Classification. Particles are classified according to size and distribution. Screen analysis is the most convenient way to estimate the size of irregular particles. The openings in a series of screens are measured, and any particle which falls through one screen but not the next is said to be in the range of the measured screen openings. The average particle diameter for the group is the average of the screen opening measurements. This technique can be used to classify many kinds of irregularly shaped particles. *Sphericity* is one measure which accounts for the amount of gas-solid contact for irregularly shaped particles. Sphericity is the ratio of surface area of a sphere with the same volume to the actual surface area of the particle. For spherical particles the sphericity is 1, and for irregular particles it is between 0 and 1.

Geldart (1986, pp. 34-46) has suggested categories based upon the premise that particles in certain size ranges behaved in similar manners when fluidized. He developed a scheme of classifying particles according to their density and size, and predicting their behavior when fluidized. See Figure 5 (from Kunii and Levenspiel, 1991, p. 78) for details of density and

size ranges for the Geldart groups.

The Geldart C group includes cohesive or very fine particles. These are very difficult to fluidize since their inter-particle forces are generally greater than the fluid drag force. There is poor particle mixing, and poor heat transfer. An example of group C particles is flour.

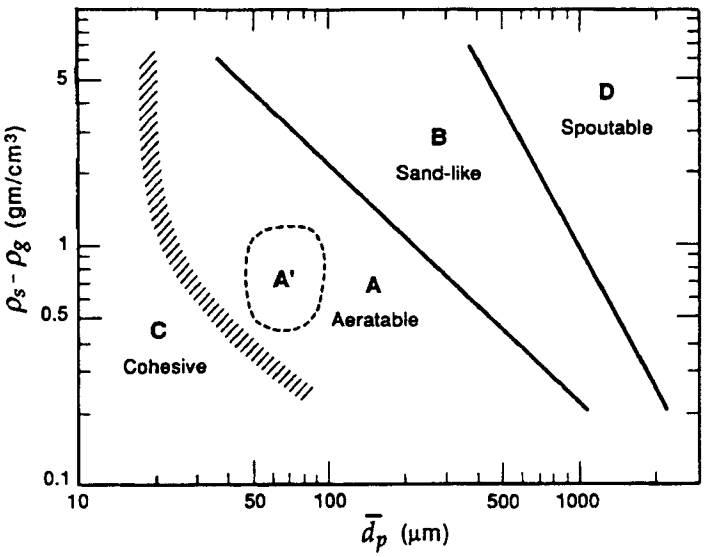

Figure 5: Geldart classification of particles.

Aeratable particles form as group A. These particles fluidize easily even though significant inter-particle forces are still present. The minimum bubbling velocity may be well above the minimum fluidization velocity, and smooth fluidization is common for fine powders. When these particles do aggregatively fluidize, even a few bubbles cause gross circulation of solids. Bubbles rise faster than the fluidizing fluid. Fluid Catalyst Cracking (FCC) catalyst particles are generally in this group.

The next group is B, the sand-like particles. They differ significantly from group A particles since they have negligible inter-particle forces, and little circulation without bubbles. Bubbles form almost as soon as minimum

fluidization velocity is exceeded, and these bubbles grow very large. There is little gas flow through the bubbles as they rise.

Finally, large and dense particles are in group D. These are called spoutable particles, since this is often the only way they can be fluidized. Bubbles coalesce rapidly and become quite large, causing erratic bed behavior with bubbles violently erupting at the surface. Bubbles rise more slowly than the fluidizing gas. Much gas is required to fluidize these systems, which is another reason that spouting rather than bubbling fluidization is often observed. Roasting coffee beans and drying grains and peas are group D processes.

Although the larger group D particles are of interest in this work, the similar characteristics of group B particles must also be considered. There is no sharp boundary dividing the groups. One measure of where in the range a solid lies is how spoutable it is. The more spoutable, the closer to the D regime it is. Another measure is the bubble rise velocity relative to the velocity of the fluidizing fluid. If only a few of the bubbles move slower than the rest of the gas, the solid behaves like a group B solid. On the other hand, if the majority of the bubbles rise more slowly than the gas, the solid is more like a group D solid. The particles used in this study are close to the group B-group D boundary, so although they are group D particles, they do share some group B characteristics.

Analytical Models

Idealizing the behavior of fluidized beds can be useful in making predictions about performance. If an accurate model for bubble characteristics can be developed, it can be used to estimate the performance of a fluidized bed or to design a better bed.

One model of a fluidized bed hydrodynamics is the two phase model (Davidson, 1963). The emulsion or gas and particle phase is seen as separate from the bubble phase. Excess gas flow is defined as all gas flow above that required for minimum fluidization. The assumption is that all excess gas goes to forming bubbles, and the emulsion phase remains at minimum fluidization conditions. The two phases are treated as distinct, which enables the modeling of bubbles in a "liquid". The use of this concept will produce relations that can be used to predict bubble behavior.

From experiment, several researchers (Botterill, 1975, p. 26; and Kunii and Levenspiel, 1991, p. 116) have determined that bubble rise velocity is mainly a function of bubble size. Davidson, etc.(1963, p. 25) have developed and verified the relation

$$U_b = k\sqrt{g\, d_b} \qquad (1)$$

where k = 0.711 from experiment. Bubble rise velocity is seen to increase with bubble diameter. If the bubble size can be predicted accurately, a typical rise velocity for that bubble can be predicted.

Bubble size increases with height above the distributor. Some

researchers (Botterill, 1975, p. 29) have found this increase to be nearly linear. Bubble size also increases with excess gas velocity. Rowe (1976) gives a formula for bubble size as a function of excess gas velocity and height above the distributor.

$$d_B = g^{-\frac{1}{4}} (h+h_o)^{\frac{3}{4}} \sqrt{U_o - U_{mf}} \qquad (2)$$

Note that the excess gas velocity is a two-phase-theory concept. The term h_0 is some reference distance below the distributor, and h is the distance of the bubble above the distributor. This relation will give a typical bubble size as a function of height above the distributor at a particular flow rate.

Experimental Method

The hydrodynamics of a bed with group D particles is of particular interest. Bubble characteristics such as shape, size, rise velocity, and frequency were studied as functions of particle size and superficial gas velocity. Both an empty bed and one with one or three internal surfaces were considered. When internals were present, their height above the distributor was varied. Results were compared with existing theories, as well as with similar research, and some relations for predicting bubble behavior in a fluidized bed were developed.

Apparatus. The test apparatus consisted of a flow delivering portion, and the fluidized-bed test section, as shown in Figure 6

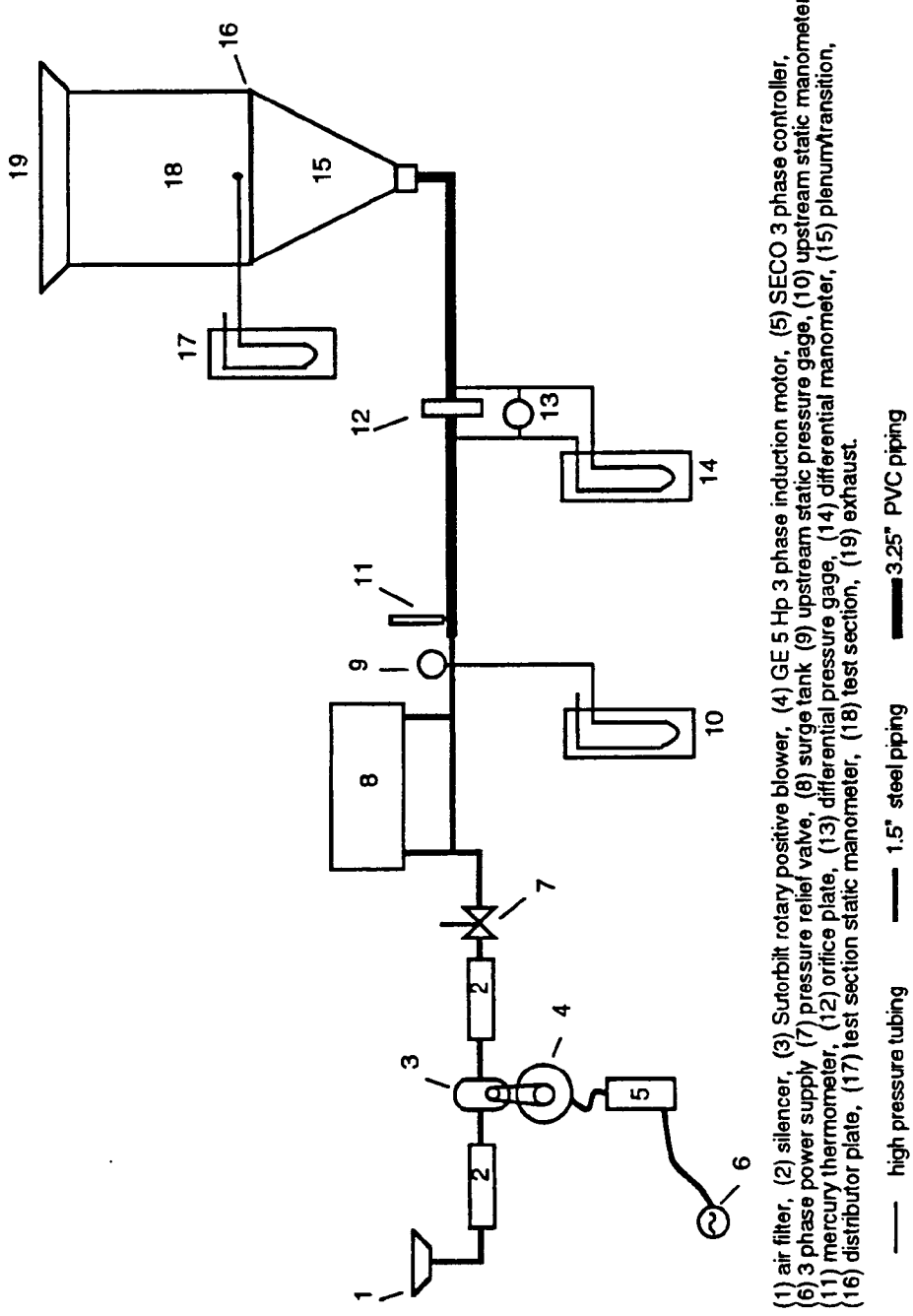

Figure 6: Fluidized bed apparatus.

(Kopczynski, 1991). A roots blower delivered the flow. This type of positive displacement pump can deliver the required flow for this system with high pressure requirements (up to 120 centimeters of water). A controller was used to adjust blower speed which controlled the amount of flow delivered to the test section. Several feet of 3-inch (7.62-cm) nominal diameter pipe and an expansion chamber were used to direct the flow to the test section. A plenum chamber was used to help damp out unsteady components of flow developed by the blower. An orifice flow meter was used to measure the flow rate. Since the loaded blower often pre-heated the air, the temperature in the duct was recorded and incorporated into the velocity calculation.

The air flow was directed to the distributor and test section. The distributor is a perforated plate, with holes 3/8 inch (0.95 cm) in diameter, and a hole spacing of 1 inch (2.54 cm) on center, which leaves about 5% of the area of the plate open for flow. This plate develops sufficient pressure drop at the desired operating conditions to ensure uniform flow into the bed.

The actual bed is 27 inches (68.5 cm) long, 1.25 inches (3.18 cm) wide, and 18 inches (45.7 cm) high, although only 12 inches (30.5 cm) of particles were tested at a time. The front wall of the test section is made of glass to permit visual observation of bed behavior. The purpose of the thin bed is to minimize three-dimensional effects. A pressure tap placed in the bed just above the distributor allowed measurement of the bed pressure drop, which enabled quick location of the point of minimum fluidization. Particles were

placed in the test section, and a screen cover was secured to minimize particle loss. To evaluate the effect of internal surfaces, several 2-inch (5.1-cm) diameter solid cylinders were placed in the bed with their axes perpendicular to the front glass to simulate tubes running through the fluidized bed.

Experiments. The visual study of the fluidized bed was accomplished using a video camera. The camera and tripod were set up to view the front glass face of the test section in the region of interest. A grid was placed on the glass to enable measurements to be taken from a video recording. The bubbling bed of particles was recorded, and reviewed in slow motion.

For this experiment, three sets of particles were studied, as listed in table 1. For each case, at least three velocities were used. The dimensionless velocity, U_o/U_{mf}, which is the ratio of superficial fluid velocity to the minimum fluidization velocity, was set near those listed in the table.

particles	size range (millimeters)	avg. diameter (millimeters)
A	1.18 - 1.70	1.44
B	1.70 - 2.00	1.85
C	2.00 - 2.36	2.18

U_o / U_{mf}
1.2
1.4
1.6

Table 1: Particle sizes and flow rates used in this research.

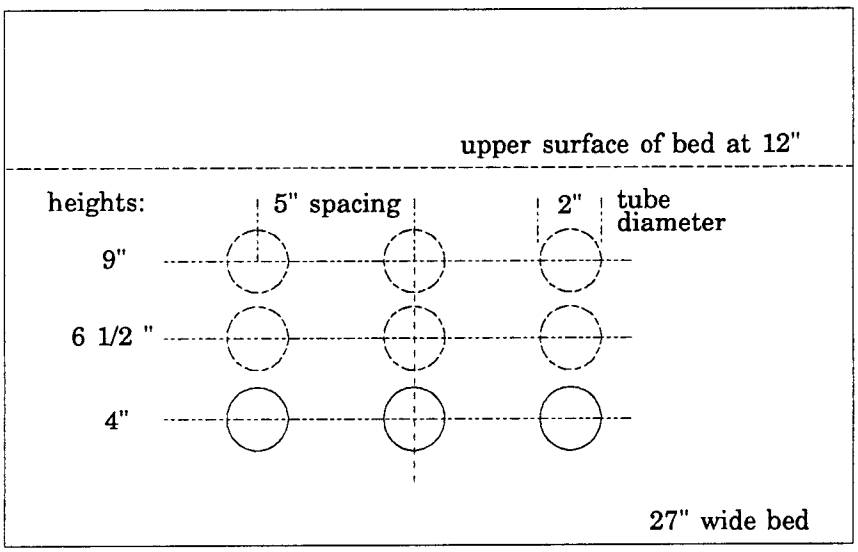

Figure 7: Internal surface location in fluidized bed test section.

Internal surfaces were located at 4 inches (10.2 cm), 6 1/2 inches (16.5 cm), and 9 inches (22.9 cm) above the distributor plate. Both one and three surfaces, spaced 5 inches (12.7 cm) apart at their centers (L/d = 2.5), were used (see figure Figure 7).

The viewpoint of the camera dictated where measurements would be taken. Both a close up view and a wide view were shot for each case. For the case with no internals, the bed was viewed in the range from 4 to 8 inches above the distributor. When internal surfaces were videotaped, the bed was viewed just above the cylinders.

Both qualitative and quantitative information were gathered. First

visual observations and qualitative information were recorded. Observations were made both during the actual experiment while videotaping, and while viewing the videotape at reduced speeds or frame by frame. Close up views were used to study bubble shape and interaction. Wide shots were useful in evaluating gross bubble behavior in the bed.

Actual measurements of bubble size, rise velocity, and frequency were also made. A close up view of the bed was used for bubble size and velocity measurements. A bubble near the center of the view with a regular shape was chosen. Bubbles that were interacting or had transverse effects were avoided. In a particular frame of the tape, where a suitable bubble was found, the number of squares occupied by voids was counted. This number is directly related to bubble size. The grid had 1 inch (2.5 cm) major divisions, and 1/4 inch (0.64 cm) minor divisions, so each square contained 1/16 square inch (0.16 cm^2) of area. For each case, 5 bubbles were read, and their sizes were averaged together to give an average bubble size and standard deviation.

Velocity was also determined from this close view of the bed. First, a stable point on the bubble, such as the stagnation point, was chosen. The number of squares this point on the bubble crossed vertically in a particular number of frames was recorded. The bubble was viewed through at least three frames where it did not interact with other bubbles. From this measurement the rise velocity of the bubble was calculated. The average

bubble rise velocity was computed from 5 individual bubble readings.

The frequency measurements were made from a wider view of the bed. For a certain number of frames, or period of time on the tape, the number of bubbles that crossed at a particular height was recorded. From these measurements frequency was computed.

Results and Discussion

First the results from the empty bed case will be discussed. These will be compared to the results with internal surfaces to determine their effect on the hydrodynamics. All bubble characteristics are plotted against normalized fluid velocity to facilitate comparison. A linear regression fit was made for the results to show general trends.

Empty Bed Studies

To begin the study of bubble characteristics in an empty bed, the observed general bubble behavior will be examined. Then bubble shapes that were observed will next be examined. Subsequently, data for bubble size, rise velocity, and frequency will be discussed. Finally, these results will be compared to the analytic relations discussed earlier.

General Behavior. The general bubble behavior in an empty bed was observed to be similar to that described by the references (Kunii and Levenspiel, 1991, p. 145-150; Botterill, 1975, p. 20-35). Small bubbles formed at the distributor, rapidly coalesced and formed the spanwise voids characteristic of large-particle beds. The length of these voids was on the order of half the bed width. Lower flow rates produced thinner voids which remained intact until they were very high in the bed, as much as 6 inches (15.2 cm) above the distributor. Eventually, these cavities were seen to

reach a level where a sudden transition to the spherical-cap shaped occurred. Once a bubble became large enough, it continued to rise and remain fairly stable, unaffected by other bubbles.

When bubbles first formed at the distributor, they coalesced and rose side by side. After the spanwise voids became unstable, a principal bubble was formed in each region. One bubble took all of the excess flow and drew smaller bubbles into it. Other neighboring bubbles actually slowed down until the principal bubble passed by. The larger bubble may temporarily be a path of less resistance, which means less flow for other bubbles, which would then shrink.

Bubble Shape. Bubble shape was affected greatly by interaction between bubbles. When bubbles coalesced or split their spherical-cap shape was temporarily distorted. When the bubble no longer had a smooth upper surface, its velocity decreased (see Figure 8).

Bubble Size. Bubble size was observed to increase with height in the bed. Bubble size also increased with flow rate and particle size, as seen in Figure 9. To show the range of bubble size measurements, error bars are

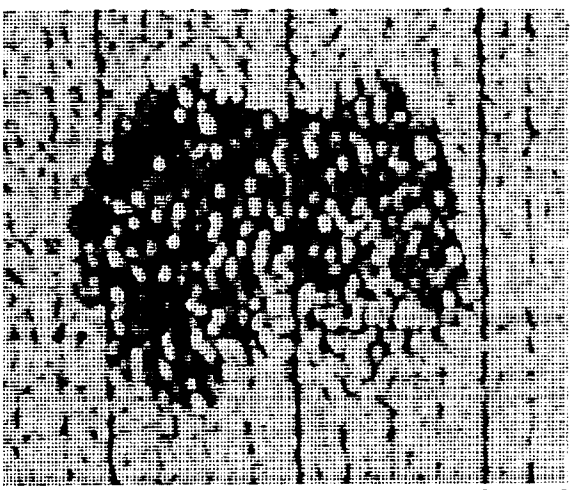

Figure 8: Spherical-cap shaped bubble.

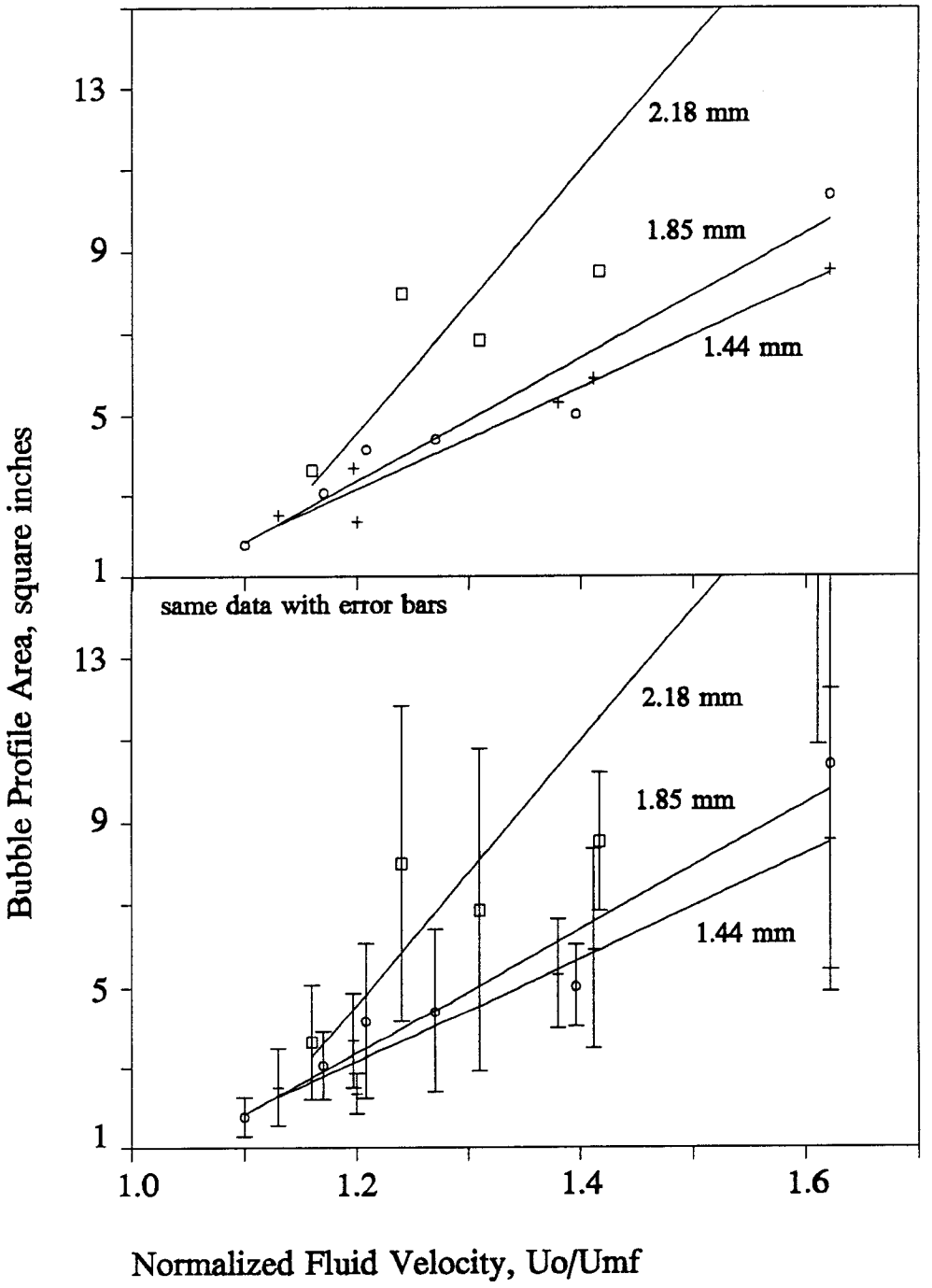

Figure 9: Bubble profile area in an empty bed.

included in the lower portion of the figure. The spread in the readings also increased with fluid velocity. Even at high flow rates, small bubbles can still be found.

Bubble Rise Velocity. One may note that the bubbles rise much more slowly than the superficial fluid. Figure 10 shows that bubble rise velocity increases with flow rate. Error bars are also shown to give an idea of the spread in the velocity measurements. There is considerable uncertainty at the high flow rates, which has a large effect on the linear regression fit. Bubble velocity probably does increase with particle size, especially since it primarily depends on bubble size. The variation of bubble velocity with fluid velocity for the 2.18 mm particles is surprisingly linear and has low error.

Bubble Frequency. Bubble frequency varies with superficial velocity and particle size. Figure 11 shows that bubble frequency decreases with increasing height in the bed. Trends indicate bubble frequency increases slightly with increasing flow rate, except for the data from the 4-inch height in the bed. In the region of the spanwise voids where bubbles rise side by side, larger bubbles at higher flow rates may become indistinguishable, reducing the number of bubbles rising in a given time period. Bubble frequency decreases with increased particle size, although the larger two particle sizes show very small differences. Note that the data points lie in a wide range, and the regression fit may not be a very

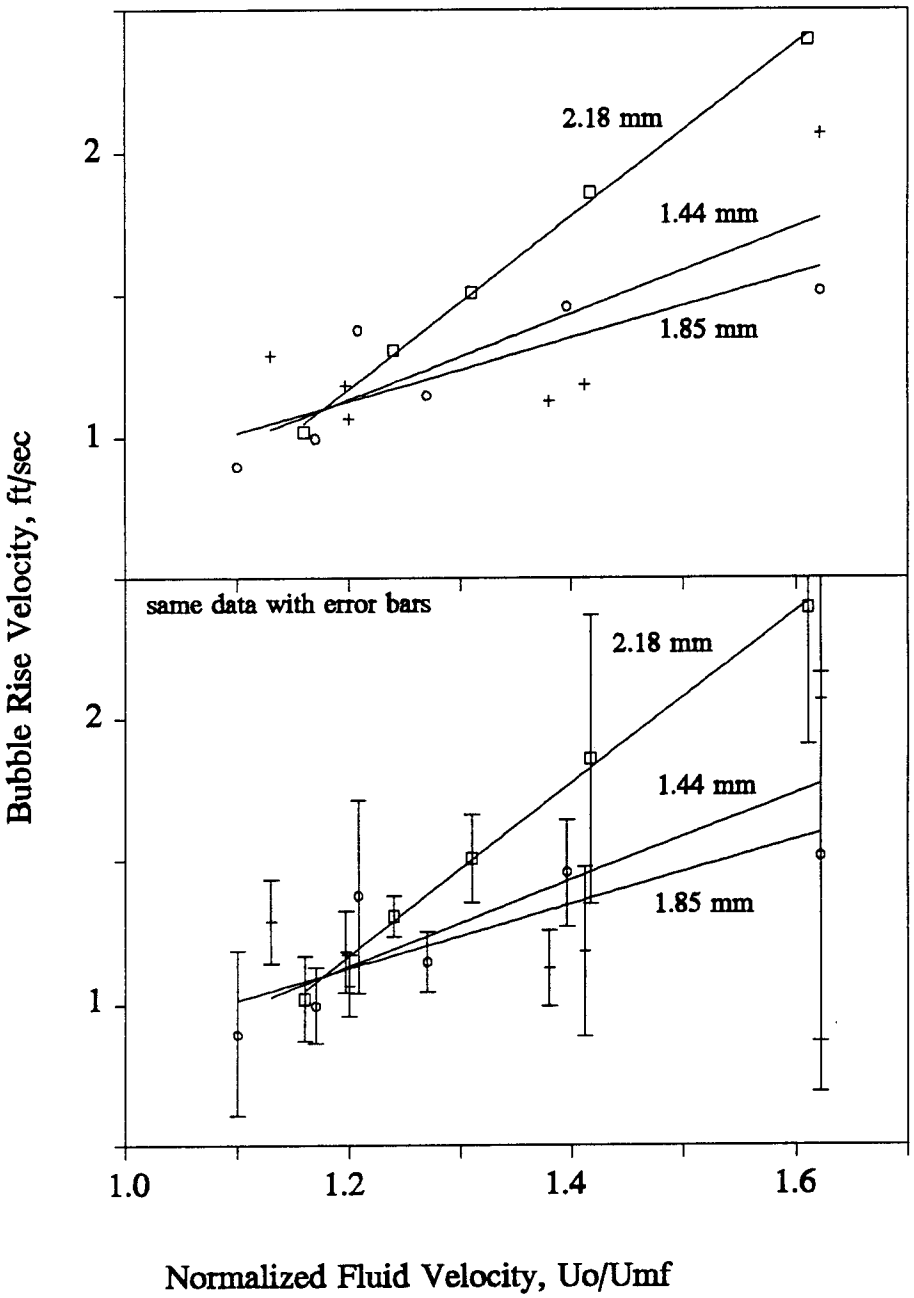

Figure 10: Bubble rise velocity in an empty bed.

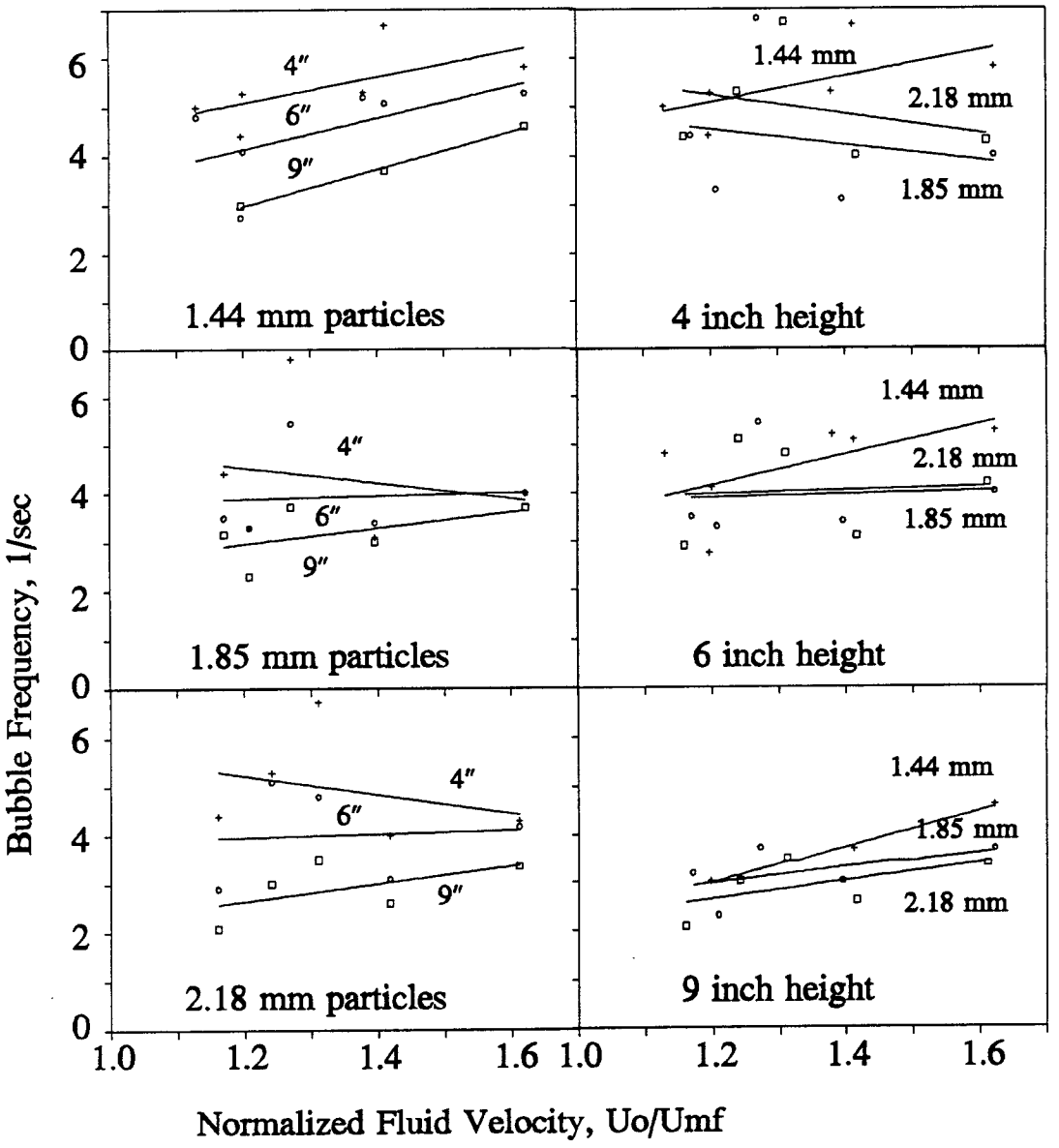

Figure 11: Bubble frequency at several heights in an empty bed for three particle sizes.

good representation of the trends.

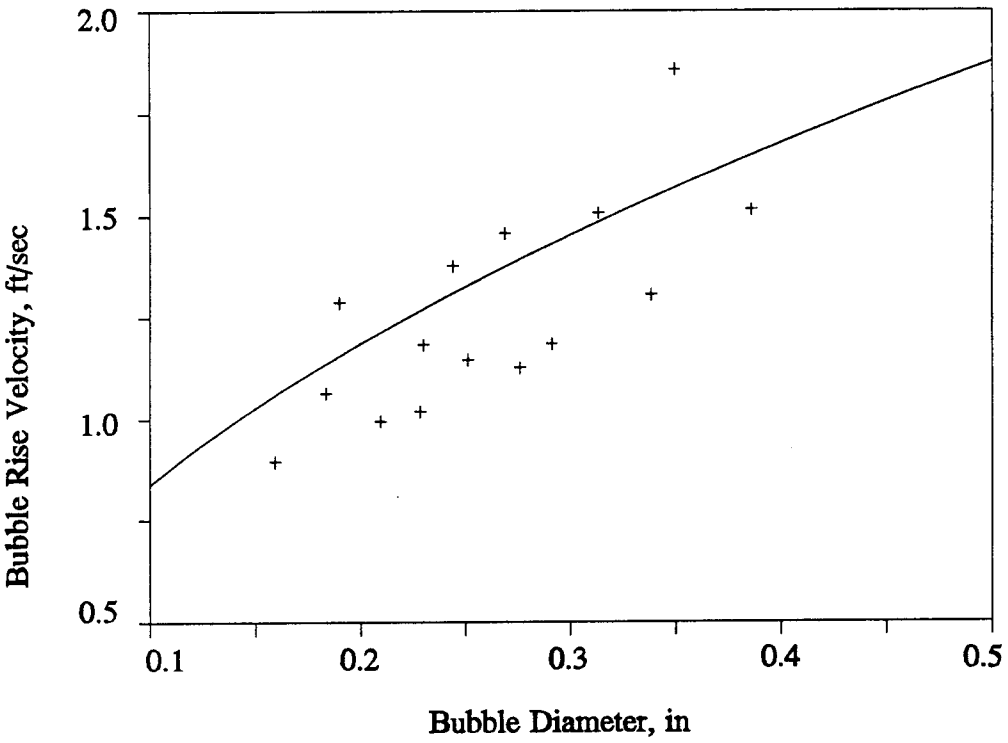

Figure 12: Bubble rise velocity as a function of bubble diameter.

Analytic Comparison. Consideration will now be given to comparing data with the analytical models presented earlier to see if bubble velocity and bubble size can be predicted from the equations. For bubble rise velocity, U_b, a linear regression fit through the origin was performed with rise velocity as the dependent variable, and $(g\ d_B)^{1/2}$ as the independent variable. This gives an estimation of the proportionality constant in equation 1. The data were plotted with equation (1) Figure 12. The data follow the same trend as the curve. This appears to be a valid way of predicting bubble rise velocity for bubbles of a given size.

This procedure was repeated for the relation between bubble size and excess velocity. The proportionality constant, $(h_o + h)^{3/4}$ was determined using bubble diameter as the dependent variable and the remaining terms in the form, $g^{-1/4}(U_o - U_{mf})^{1/2}$, as the independent variable. Bubble diameter

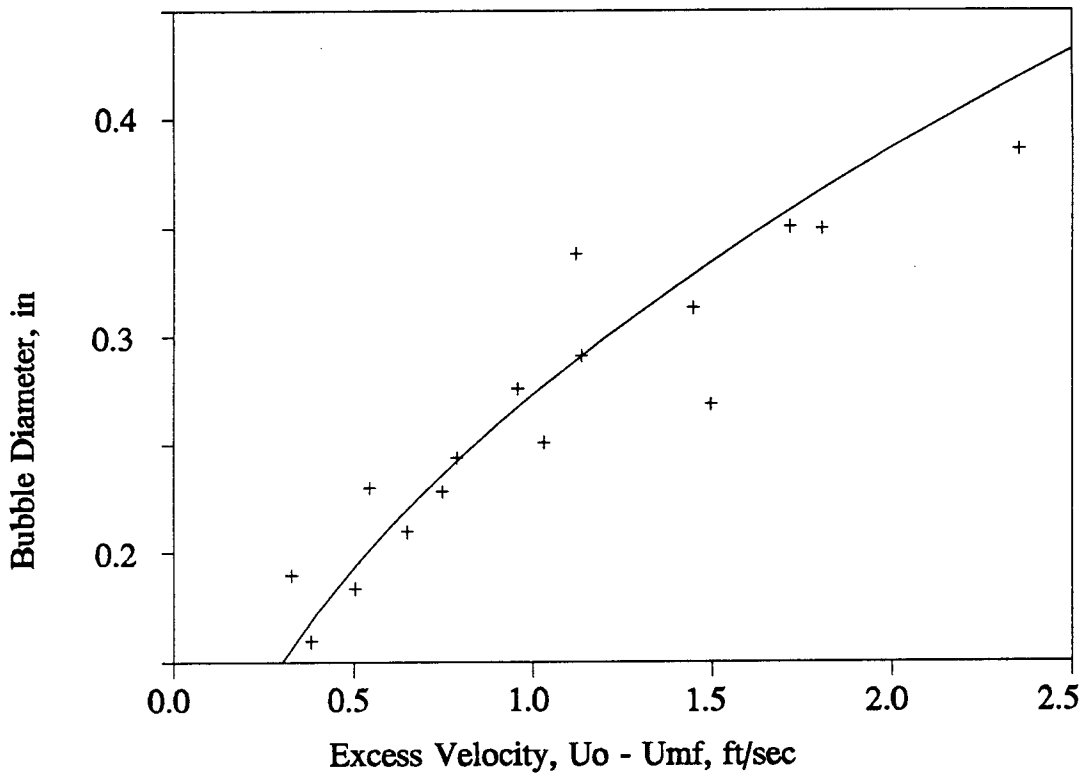

Figure 13: Bubble size as a function of excess velocity.

is plotted against excess velocity in Figure 13, and both data and equation (2) are shown. Again, the data follow the general trend predicted by analysis. If h_o can be experimentally determined, then bubble size can be predicted at a certain flow rate and height in the bed, and a hydrodynamic model could be developed.

Bed With Internal Surfaces

Bubble characteristics are now considered for a bed with internal surfaces. These are compared to the results for a bed with no internals.

General Behavior. Internal surfaces affect the formation, path, size, velocity, and frequency of bubbles, and thus affect hydrodynamic behavior. These effects change when the position of the surfaces in the bed is varied. If the internal surfaces, in the form of tubes, are located 4 inches above the distributor, they are located in the region where spanwise voids would exist in an empty bed. Voids form at the lower surface of the tube and remain, growing and shrinking in an oscillatory fashion. If the flow rate is low or the tubes are close together, the voids near the tubes form a bridge between the tubes. These bridges block the rise of bubbles and impede the circulation of particles downward. Above the tubes, no spanwise voids exist, only bubbles of a more typical shape. The tubes appear to disrupt the stability of these cavities prematurely.

Tubes affected hydrodynamics differently when they were placed in a region above the point of transition to bubbles. For this study such behavior was exhibited at the 6-1/2 inch height. Bubbles were attracted to the tubes as they rose, and frequently interacted with the surfaces. Voids below the surface developed from bubbles which came into contact with the tubes. Bridges also formed, but were not as stable and were not formed as frequently. At lower velocities, bubbles became laterally displaced from

their original path when they encountered a tube. At higher superficial velocities, a bubble moved around a tube, remaining on its original path. Tubes had less effect on bubble path at higher velocities.

When the tubes were located well above the region where distributor effects were present, for example at the 9-inch level, the tubes had still less effect on bed hydrodynamics. The bubbles arriving at the tubes were larger, more stable, and less likely to form a void at the lower surface of the tube. More often, they rose past or adjacent to the tube without being significantly affected. Bridging was unlikely, although it did occur at low flow rates or when the tubes were quite close together.

Bubble Shape. Bubbles still had their characteristic spherical-cap shape in the bed with internal surfaces when they were not interacting. In fact, spherical-cap shaped bubbles formed earlier if the spanwise voids were broken up prematurely. When bubbles interacted with lower tubes, they formed a void that persists under the tube, and their shape conformed to the lower side of the tube. Once a bubble was again formed from this void, it returned to the spherical-cap shape. Tubes that were higher in the bed only temporarily distorted the bubble as it passed by or over the tube. However, the bubbles returned to their stable spherical-cap shape.

Bubble Size. For the case of a fluidized bed with three internal surfaces, there appears to be no difference in bubble size between the three heights in the bed where the surfaces were located (see Figure 14). Bubble

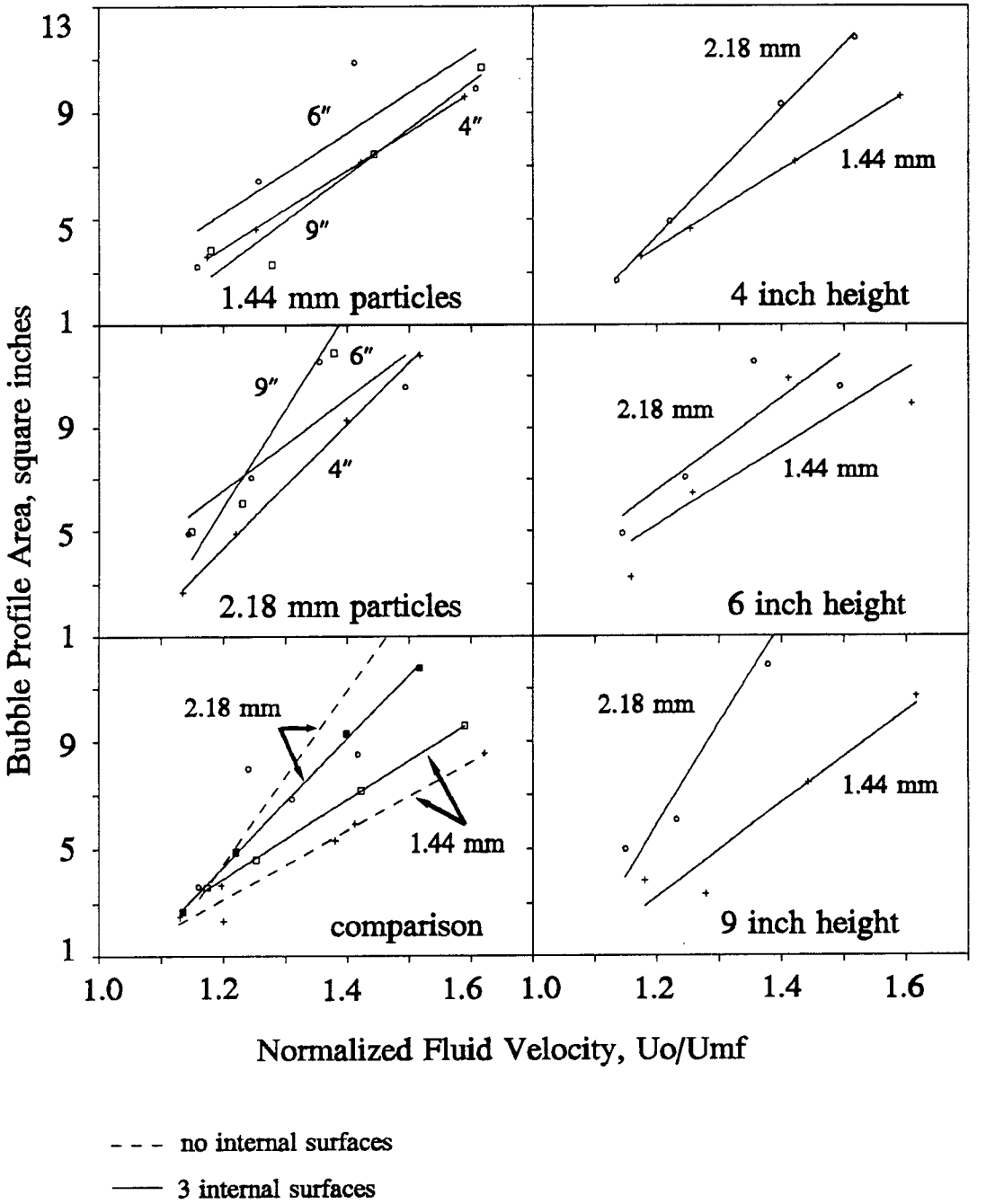

Figure 14: Bubble profile area in a bed with three internal surfaces at several heights for various particle sizes.

size increased with flow rate, but it seems to be related only to a given tube spacing, regardless of what size the bubble would be in an empty bed at that height. The larger particles do produce larger bubbles even with internals. Including the internal surfaces in the bed appears to have little effect on the way particle size affects bubble size.

Bubble Rise Velocity. Bubble rise velocity increased with fluid velocity for the case of three internal surfaces (see Figure 15). However, there is no distinct pattern for changes in bubble rise velocity with the height of the internal surfaces in the bed. For the smaller particles, bubbles at 6 1/2 inches and 9 inches are almost indistinguishable, while the 4-inch-high emerging bubble velocity is different. With larger particles, the 4 inch and 6 1/2 inch bubbles rise similarly, while the 9-inch level bubbles behave differently. Bubble rise velocity does increase with particle size. Discounting one data point, the linear regression line for the 2.18 mm particles would be reasonably clear, and the trend of increasing bubble rise velocity with increasing height of tubes would be reasonably consistent. Comparing the bubble rise velocities of an empty bed and a three-tube case, the presence of the surfaces is seen to slightly increase the rise velocity. Other trends remain unchanged, such as an increase with flow rate.

Frequency of Emerging Bubbles. Frequency of emerging bubbles from the tubes increases with flow rate also (see Figure 16). No real trend occurs when surface height is varied, except that there seem to be more

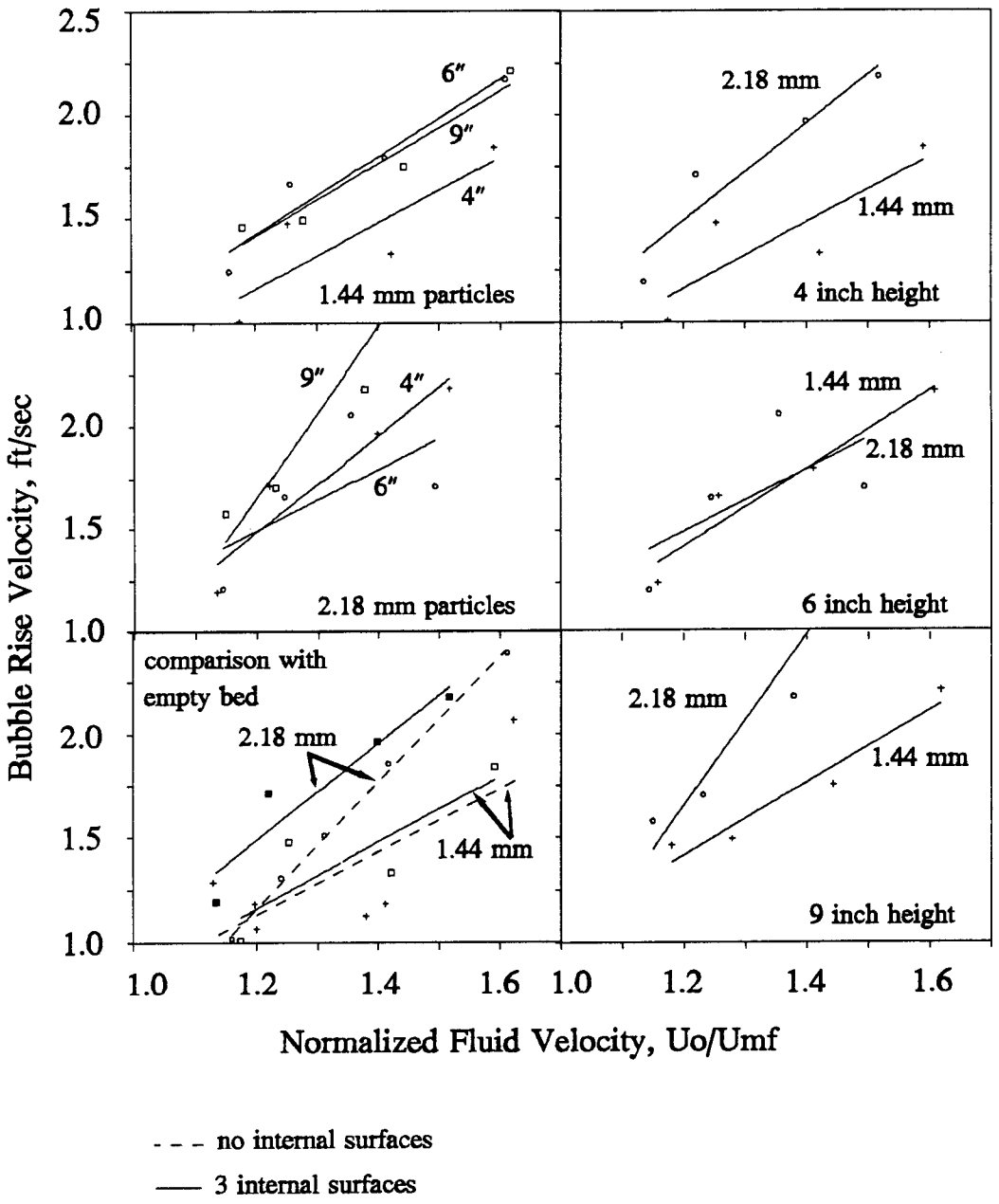

Figure 15: Bubble rise velocity for a bed with three internal surfaces at various heights with three particle sizes.

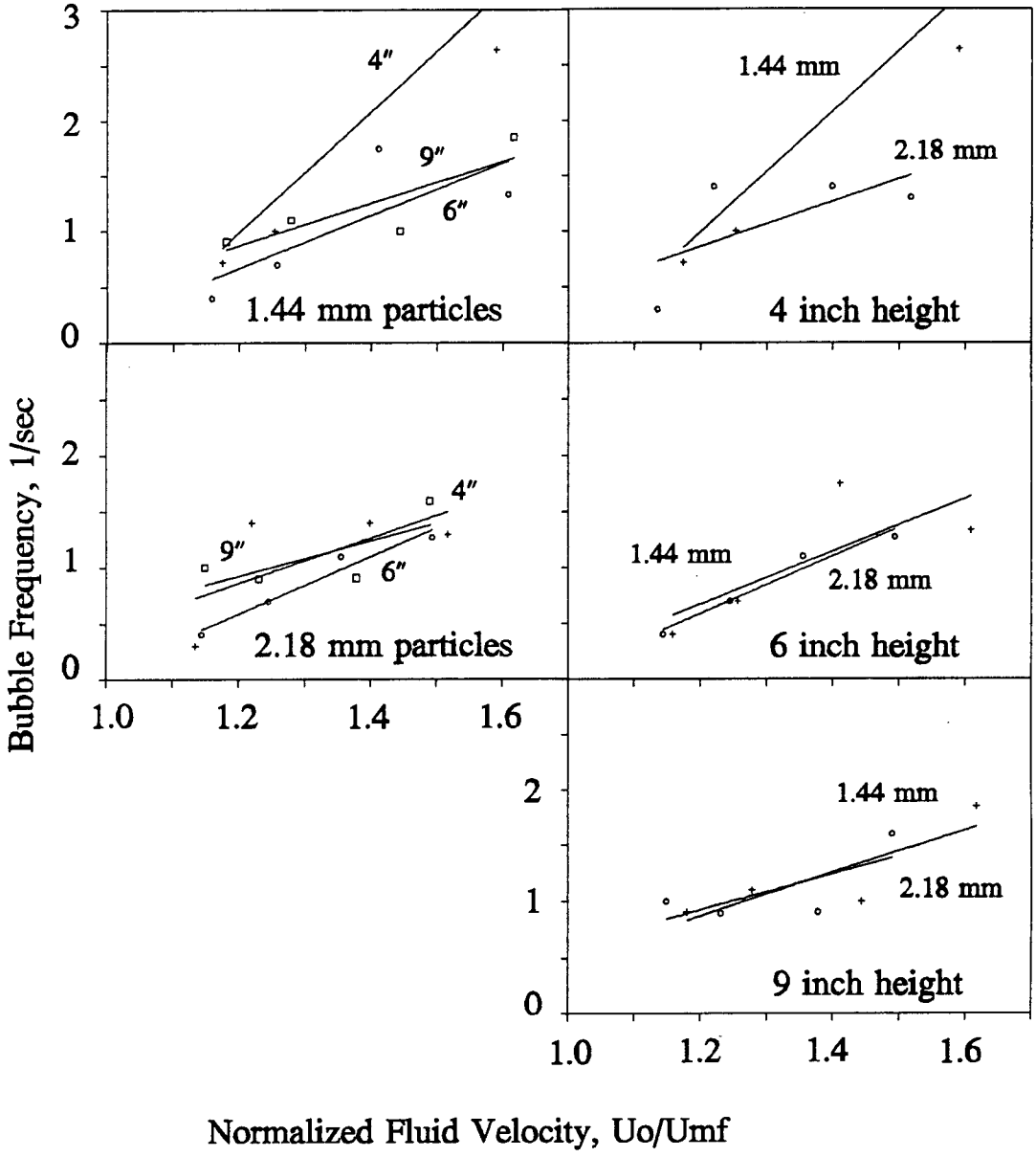

Figure 16: Bubble frequency in a bed with three internal surfaces at several heights with three sizes of particles.

bubbles emerging from the surfaces located at the 4-inch level for the smaller particle case. From two of the graphs, particle size appears to have little effect on bubble frequency. This may discount the 1.44 mm particle point at 4 inch-tube height and at 1.6 U_o/U_{mf}. If the slope of this linear regression were more like the 2.18 mm line, this would reinforce that there is little change in frequency when the height of the tubes is varied.

When the cases with internal surfaces are compared to those for the empty bed, a general trend of decreasing bubble frequency with increasing height in the bed shows up (see Figure 17). Also, bubble frequency does increase slightly with superficial velocity. Note that the empty bed cases all exhibited much higher bubble frequencies and are spread over a wider range than the cases with internals. Bubble frequency is affected little by particle size in the bed with internals, but frequency decreases with increased particle size in the empty bed. Note again that frequencies in the empty bed are much higher.

Percentage of Time Lower Side of Tube is Exposed. One measure of the effectiveness of heat transfer to the tubes is how frequently and over what portion of its surface the tube is touched by particles. Heat transfer to the tube is greatly reduced when a bubble is present (Botterill, 1975, p. 254-5). Generally, the upper half of the tube has a stack of stationary particles resting on it. The lower surface of the tube is often covered by a bubble. The less often these conditions occur, the better the

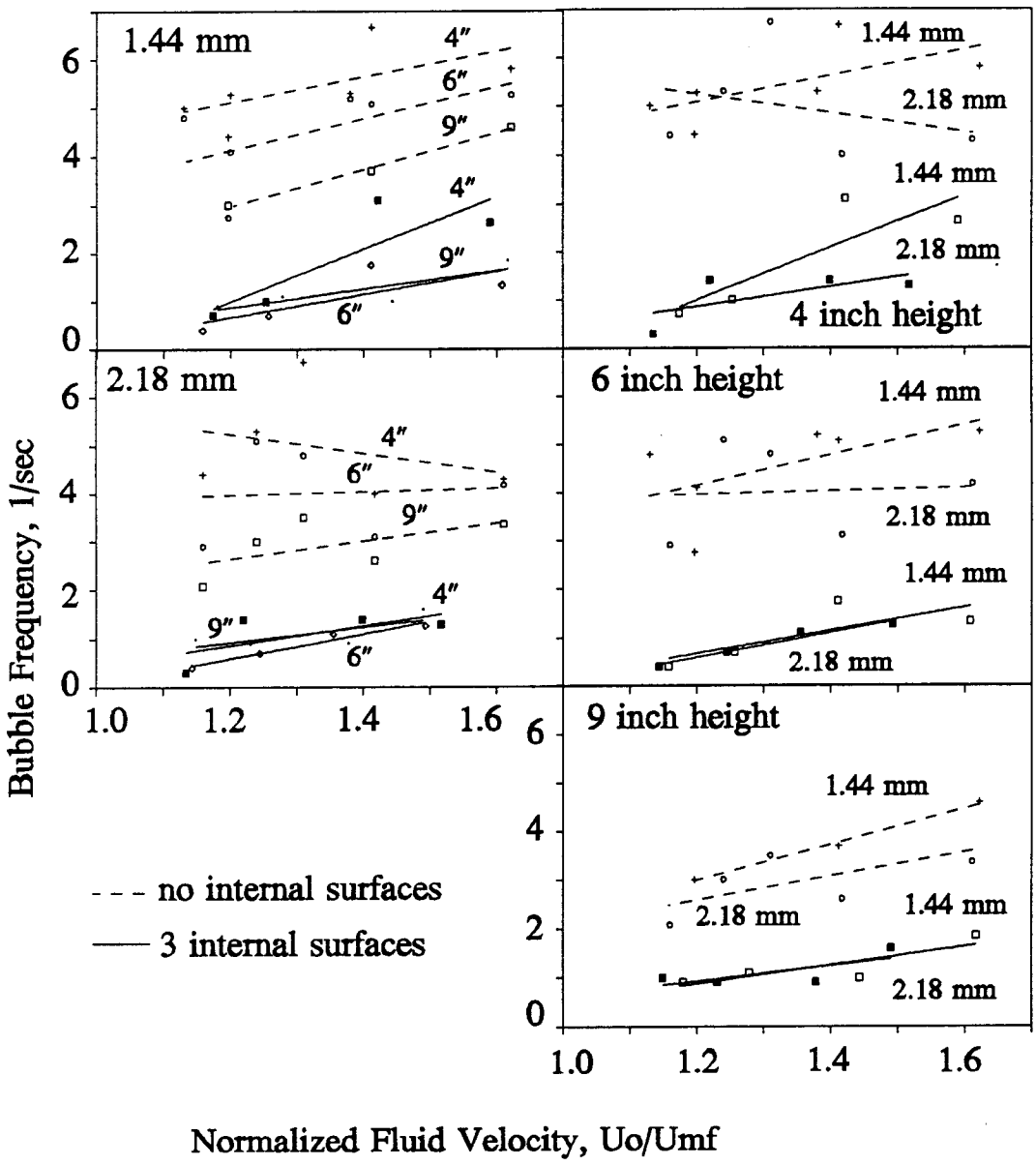

Figure 17: Bubble frequency in an empty bed compared to a bed with three internal surfaces.

the heat transfer will be.

For the cases with one and three tubes, the amount of time the lower tube surface is exposed to a bubble decreases with increased height of the tubes in the bed. The time does not appear to change appreciably with increased flow rate, and no trend seems apparent. Results are similar for both cases (see Figure 18). With larger particles there is increased time for exposure. At the 9-inch height, exposure time increased with flow rate. Such a relationship is not as clear for the operation at the other heights.

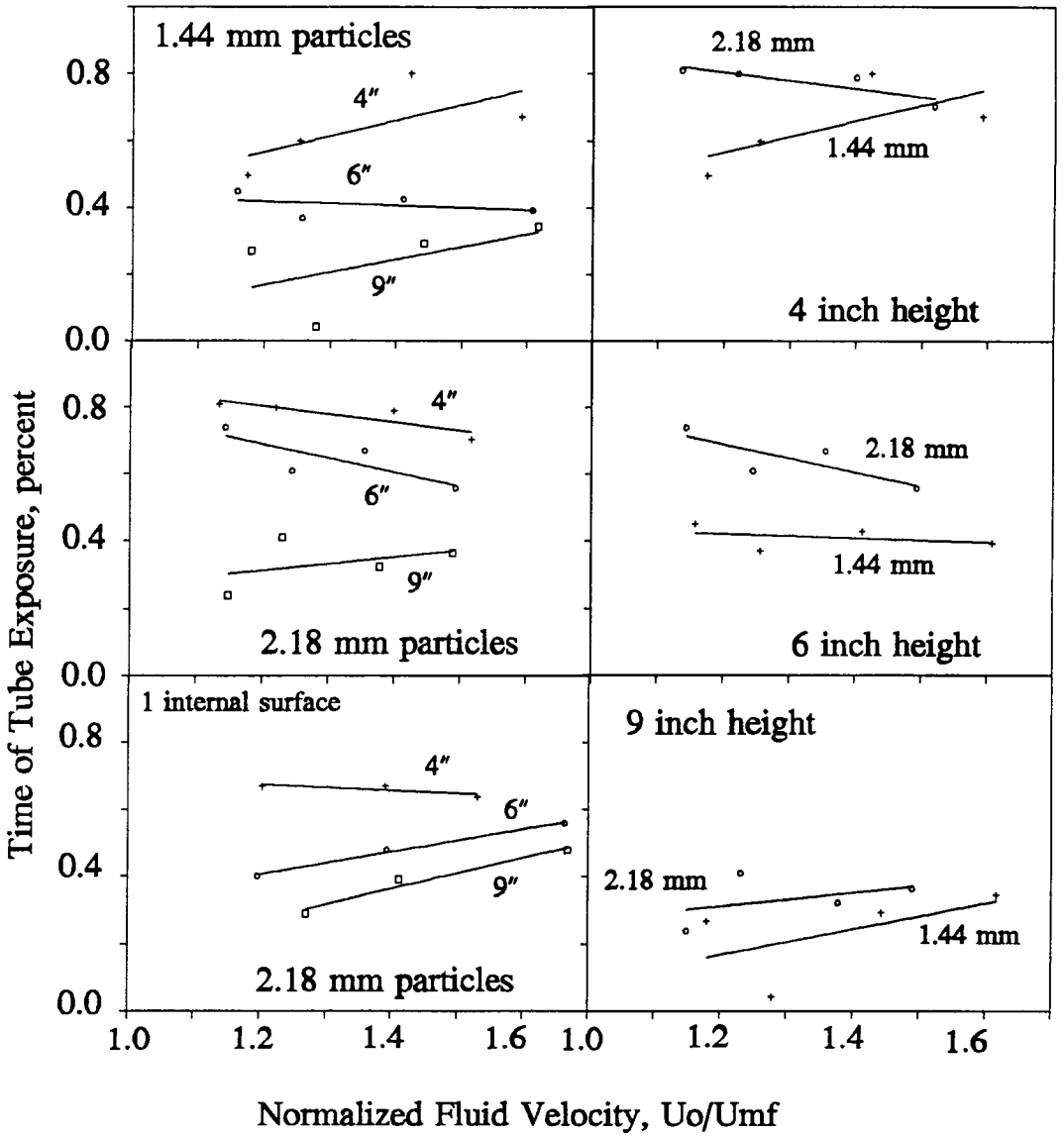

Figure 18: Percentage of time the lower side of the tubes is exposed in a bed with three internal surfaces at several heights for three particle sizes.

Conclusions and Recommendations

General Trends

Typically in a fluidized bed, bubble size, rise velocity, and frequency increase with increased superficial velocity. An increase in particle size causes an increase in bubble size and rise velocity, but a decrease in bubble frequency. The presence of internal surfaces has the effect of reducing the bubble size, rise velocity, and frequency, and also reduces the effect of changing the particle size and superficial velocity in comparison to a bed without internals. Increasing the height of the tubes in the bed also has little effect on the bubbles emerging from them, except to reduce the frequency modestly.

Observations of the amount of time lower tube surfaces were exposed suggest that the higher the tube, the more contact with the emulsion phase, and thus better heat transfer. However, a second row of tubes would see the same bubbles regardless of the first row location. Placing the tubes high above the distributor means fluidizing more particles. Since this would be accompanied by greater pressure drop and more cost, it may be more feasible to sacrifice the heat transfer of the first row and begin the tube bank at a reasonable height in the bed.

Comparison With Expected Results

Overall, the trends displayed in this study were as expected. The

general behavior and bubble shape observed matched descriptions in several references (Kunii and Levenspiel, 1991, p. 115; and Geldart, 1986, p. 54). Bubble size and rise velocity increased with flow rate, as expected. Particle size was expected to have little effect on bubble characteristics, although some trends did appear in this research.

Similar research using optical probes compare moderately well with these results (Kopczynski, 1991). In this earlier work, frequency was shown to increase with superficial velocity. Although the effect of superficial velocity on rise velocity and bubble size did not seem clear because of large scatter, an increasing trend did appear. Also, at higher superficial velocities, the scatter in the data was greater, and larger bubbles appeared while smaller bubbles also remained. Similar trends can be found in this research (refer to Figure 9, 21).

Frequency increased slightly with increasing particle size, while in the present work showed a slight decrease, but both sets displayed much scatter. No trends were apparent when particle size was varied for bubble size and rise velocity, while some modest trends appear in this research.

Recommendations for Future Research

A more automated method of acquiring data for bubble size and rise velocity would enable better correlations and allow more accurate empirical results. The development of a two dimensional histogram showing bubble size and rise velocity data might enable numerical modeling of a fluidized

bed. Improved predictions could then be made about hydrodynamics and heat transfer.

More studies should be performed on tube effects, especially with a complete first row of tubes across the bed. The bubble effects on the second and third rows of tubes are of interest, and will likely be quite different from first row tube results presented here.

Bibliography

Botterill, J. S. M., *Fluid-Bed Heat Transfer*. London: Academic Press, 1975.

Cheremisinoff, N. P. and Cheremisinoff, P. N., *Hydrodynamics of Gas-Solids Fluidization*. Houston: Gulf Publishing Co., 1984, pp. 137-206.

Davidson, J. F. and Harrison, D., *Fluidised Particles*. Cambridge: Cambridge University Press, 1963.

Geldart, D, ed., *Gas Fluidization Technology*. Chichester: John Wiley and Sons, 1986, pp. 11-95.

Godard, K. and Richardson, J. F., "Bubble velocities and bed expansions in a freely bubbling fluidised beds," *Chemical Engineering Science*, Vol. 24, 1969, p. 663-670.

Kopczynski, Sean, *Hydrodynamic Signatures of a 2-D Gas-Solid Fluidized Bed*, Masters Thesis, Oregon State University, 1991.

Kunii, D. and Levenspiel, O., *Fluidization Engineering*. Boston: Butterworth-Heinemann, 1991, pp. 1-162.

Rowe, P. N., "Prediction of Bubble Size in a Gas Fluidized Bed," *Chemical Engineering Science*, vol. 31, 1976, pp. 285-288.

Rowe, P. N. and Partridge, B. A., "An X-ray Study of Bubbles in Fluidized Beds," *Transactions of Institution of Chemical Engineers*. Vol. 43, 1965 p. T157-T175.

Watkins, S. P. and Creasy, D. E., "The Stability of Bubbles Injected into Particulate Gas-Fluidized Beds," *Powder Technology*, Vol. 9, 1974, p. 241-5.

Weihong, Luo et. al., "Measurements of Bubble and Particle Motion in a Two-Dimensional Fluidized Bed," *Proceedings of the 1987 International Conference on Fluidized Bed Combustion*, Boston: the American Society of Mechanical Engineers, 1987.

Yang, Wen-Ching et. al., "Fluidization Phenomena in a Large-Scale, Cold-Flow Model," *Fluidization, IV*, Proceedings of the International Conference on Fluidization, New York: Engineering Foundation, 1989.

Appendix

The data from this research are included in the following tables. The headings and codes listed in the tables are defined here.

DATE/RUN	Data are listed according to date it was taken and a case or run number.
D	Particle diameter in millimeters. The letter A represents 1.44 mm particles, B is 1.85 mm particles, and C is 2.18 mm particles.
H	Height above the distributor in inches at which the data was taken. A value of 0 for the case of an empty bed means the data was taken at the usual 4-inch height.
CO	Configuration of the bed. An E stands for empty bed, and a number indicates the number of internal surfaces present.
U/UMF	This is the normalized fluid velocity used.
AREA1	These five columns contain the actual bubble profile area readings for the five bubbles considered. These values are in square inches.
AREAV	This column contains the average value of the five profile areas, again in square inches.
AREASD	This is the standard deviation in the area readings.
VEL1	These five columns contain the actual bubble rise velocity readings for the five bubbles considered. These velocities are in feet per second.
VELAV	This is the average of the five bubble velocity readings, again in feet per second.
VELSD	This is the standard deviation in the velocity readings.

FE4	These three columns contain the bubble frequency measurements for the empty bed case at three heights, 4, 6, and 8 inches. These are in units of 1/second.
FEMRG	This is the frequency of bubbles emerging from three internal surfaces, in units of 1/second.
VOID%	These are values for the percent of time a void covers more than half of the lower surface of the tube.
Umf	These are the actual minimum fluidization velocities measured for each case, in feet per second.
U	These are the fluidizing velocities used in feet per second.

DATE/R	C	U/UM	D	H	AREA1	AREA2	AREA3	AREA4	AREA5	AREA	AREAS
9-3-9	E	1.130	A		2.938	1.125	1.625	3.375	3.501	2.513	0.961
9-3-10	E	1.200	A		2.688	2.188	2.688	2.750	1.438	2.350	0.499
9-3-11	E	1.380	A		5.938	3.063	4.625	6.875	6.063	5.313	1.336
1-21-10	E	1.197	A		4.438	3.188	2.563	2.625	5.625	3.688	1.180
1-21-11	E	1.412	A		3.500	7.188	3.938	4.875	10.063	5.913	2.435
1-21-12	E	1.622	A		13.250	4.125	4.375	10.688	10.375	8.563	3.661
9-3-12A	E	1.100	B		1.188	1.938	1.938	1.313	2.500	1.775	0.477
9-3-12B	E	1.170	B		4.625	2.313	3.188	2.313	2.875	3.063	0.850
9-3-13	E	1.270	B		2.688	5.313	7.625	2.000	4.375	4.400	1.996
1-21-1	E	1.208	B		5.063	1.813	3.063	3.438	7.375	4.150	1.918
1-21-2	E	1.396	B		5.063	5.563	6.625	3.875	4.063	5.038	1.010
1-21-3	E	1.622	B		5.188	15.375	17.375	6.938	7.065	10.388	4.973
9-3-1	E	1.160	C		3.625	1.250	4.938	3.125	5.250	3.638	1.432
9-3-3	E	1.240	C		3.000	11.813	11.813	9.438	3.875	7.988	3.825
9-3-4	E	1.310	C		14.313	7.313	3.938	4.500	4.188	6.850	3.924
1-30-25	E	1.417	C		8.063	7.063	9.625	6.688	11.188	8.525	1.675
1-30-26	E	1.611	C		20.000	15.500	20.500	34.000	7.500	19.500	8.620
10-4-2	3	1.174	A	4	5.375	2.563	4.500	3.125	2.438	3.600	1.150
10-4-3	3	1.253	A	4	4.250	3.625	7.000	4.563	3.750	4.638	1.229
1-21-13	3	1.422	A	4	6.188	13.313	3.375	5.625	7.313	7.163	3.332
1-21-14	3	1.590	A	4	9.625	7.563	5.688	12.188	12.938	9.600	2.731
10-4-5	3	1.158	A	6	4.750	3.438	3.563	2.625	1.813	3.238	0.984
10-4-6	3	1.257	A	6	7.188	4.500	9.188	4.438	6.938	6.450	1.796
1-21-15	3	1.411	A	6	8.375	12.438	14.438	8.250	10.938	10.888	2.378
1-21-16	3	1.608	A	6	6.75	7.875	13.313	9.563	8.875	9.907	2.056
10-4-8	3	1.180	A	9	7.000	3.313	3.625	2.000	3.313	3.850	1.672
10-4-9	3	1.278	A	9	3.313	2.813	4.188	2.813	3.478	3.321	0.508
1-21-17	3	1.443	A	9	8.313	5.536	8.188	9.750	5.438	7.445	1.691
1-21-18	3	1.617	A	9	14.000	11.000	10.000	7.500	11.000	10.700	2.088
10-4-11	3	1.135	C	4	1.875	1.188	3.313	3.313	3.813	2.700	0.996
10-4-12	3	1.220	C	4	4.188	3.938	8.563	3.875	3.938	4.900	1.834
1-30-23	3	1.399	C	4	11.250	11.438	8.250	8.000	7.563	9.300	1.684
1-30-24	3	1.517	C	4	10.438	15.688	9.563	11.813	11.500	11.800	2.101
10-4-14	3	1.144	C	6	6.000	8.375	3.875	2.938	3.313	4.900	2.035
10-4-15	3	1.245	C	6	5.750	2.188	12.313	8.875	6.188	7.063	3.379
1-30-21	3	1.355	C	6	8.063	9.063	17.188	9.688	13.750	11.550	3.419
1-30-22	3	1.493	C	6	11.938	8.625	12.375	12.313	7.563	10.563	2.049
10-4-17	3	1.149	C	9	3.688	4.063	7.813	4.563	4.813	4.988	1.465
10-4-18	3	1.231	C	9	3.250	10.250	3.500	8.500	4.750	6.050	2.817
1-30-19	3	1.378	C	9	6.000	8.500	13.000	15.000	17.000	11.900	4.079
1-30-20	3	1.490	C	9	13.000	11.500	26.000	21.000	17.000	17.700	5.307

DATE/R	C	U/UM	D	H	VEL1	VEL2	VEL3	VEL4	VEL5	VELAV	VELSD
9-3-9	E	1.130	A		1.250	1.125	1.250	1.250	1.563	1.288	0.146
9-3-10	E	1.200	A		1.250	1.042	1.000	0.938	1.094	1.065	0.106
9-3-11	E	1.380	A		1.375	1.042	1.094	1.125	1.000	1.127	0.131
1-21-10	E	1.197	A		1.250	1.250	1.000	1.042	1.375	1.183	0.141
1-21-11	E	1.412	A		1.406	0.781	0.875	1.406	1.458	1.185	0.294
1-21-12	E	1.622	A		3.333	4.068	0.536	1.250	1.146	2.067	1.376
9-3-12A	E	1.100	B		0.781	1.458	0.781	0.625	0.833	0.896	0.290
9-3-12B	E	1.170	B		1.094	0.833	0.833	1.125	1.094	0.996	0.133
9-3-13	E	1.270	B		1.094	1.354	1.094	1.071	1.125	1.148	0.105
1-21-1	E	1.208	B		1.000	1.094	1.250	1.667	1.875	1.377	0.338
1-21-2	E	1.396	B		1.250	1.250	1.458	1.667	1.667	1.458	0.186
1-21-3	E	1.622	B		1.875	0.536	1.875	1.000	2.292	1.516	0.646
9-3-1	E	1.160	C		0.938	0.951	0.833	1.125	1.250	1.019	0.149
9-3-3	E	1.240	C		1.406	1.250	1.375	1.250	1.250	1.306	0.070
9-3-4	E	1.310	C		1.500	1.458	1.667	1.667	1.250	1.508	0.155
1-30-25	E	1.417	C		1.071	2.500	1.500	2.031	2.188	1.858	0.510
1-30-26	E	1.611	C		2.500	2.344	2.917	1.500	2.708	2.394	0.487
10-4-2	3	1.174	A	4	0.938	1.042	0.938	0.875	1.250	1.009	0.132
10-4-3	3	1.253	A	4	1.406	1.016	2.292	1.406	1.250	1.474	0.433
1-21-13	3	1.422	A	4	0.714	1.354	1.667	1.042	1.875	1.330	0.418
1-21-14	3	1.590	A	4	1.500	1.458	2.188	1.875	2.188	1.842	0.318
10-4-5	3	1.158	A	6	1.250	1.458	1.667	0.982	0.875	1.246	0.293
10-4-6	3	1.257	A	6	1.406	1.500	1.667	1.875	1.875	1.665	0.191
1-21-15	3	1.411	A	6	2.292	1.875	1.563	1.875	1.375	1.796	0.313
1-21-16	3	1.608	A	6	1.250	2.500	2.500	2.500	2.083	2.167	0.486
10-4-8	3	1.180	A	9	1.875	1.042	1.667	1.250	1.458	1.458	0.295
10-4-9	3	1.278	A	9	1.094	1.458	1.458	1.563	1.875	1.490	0.250
1-21-17	3	1.443	A	9	1.250	1.667	2.083	2.344	1.406	1.750	0.410
1-21-18	3	1.617	A	9	2.292	2.500	1.875	1.719	2.656	2.208	0.359
10-4-11	3	1.135	C	4	1.458	0.781	0.938	1.667	1.125	1.194	0.327
10-4-12	3	1.220	C	4	1.667	1.875	1.875	1.667	1.458	1.708	0.156
1-30-23	3	1.399	C	4	1.500	1.875	2.500	1.458	2.500	1.967	0.459
1-30-24	3	1.517	C	4	1.328	2.500	1.875	2.708	2.500	2.182	0.510
10-4-14	3	1.144	C	6	1.667	1.406	1.250	1.000	0.729	1.210	0.324
10-4-15	3	1.245	C	6	1.250	1.406	1.875	1.875	1.875	1.656	0.272
1-30-21	3	1.355	C	6	1.875	2.188	2.500	1.719	2.000	2.056	0.270
1-30-22	3	1.493	C	6	1.458	2.344	1.667	1.500	1.563	1.706	0.326
10-4-17	3	1.149	C	9	1.094	0.938	2.292	2.083	1.458	1.573	0.533
10-4-18	3	1.231	C	9	1.250	1.875	1.000	2.500	1.875	1.700	0.528
1-30-19	3	1.378	C	9	1.875	2.292	2.500	1.875	2.344	2.177	0.256
1-30-20	3	1.490	C	9	2.813	3.333	2.708	2.917	3.333	3.021	0.263

DATE/R	C	U/UM	D	H	FE4	FE6	FE8	FEMER	%VOID
9-3-9	E	1.130	A					-	-
9-3-10	E	1.200	A					-	-
9-3-11	E	1.380	A					-	-
1-21-10	E	1.197	A		4.417	2.75	3	-	-
1-21-11	E	1.412	A		6.67	5.08	3.7	-	-
1-21-12	E	1.622	A		5.8	5.27	4.6	-	-
9-3-12A	E	1.100	B					-	-
9-3-12B	E	1.170	B					-	-
9-3-13	E	1.270	B					-	-
1-21-1	E	1.208	B		3.3	3.3	2.3	-	-
1-21-2	E	1.396	B		3.1	3.4	3	-	-
1-21-3	E	1.622	B		4	4	3.7	-	-
9-3-1	E	1.160	C					-	-
9-3-3	E	1.240	C					-	-
9-3-4	E	1.310	C					-	-
1-30-25	E	1.417	C		4	3.1	2.6	-	-
1-30-26	E	1.611	C		4.3	4.18	3.36	-	-
10-4-2	3	1.174	A	4	-	-	-	0.72	0.5
10-4-3	3	1.253	A	4	-	-	-	1	0.6
1-21-13	3	1.422	A	4	-	-	-	3.1	0.8
1-21-14	3	1.590	A	4	-	-	-	2.64	0.672
10-4-5	3	1.158	A	6	-	-	-	0.4	0.45
10-4-6	3	1.257	A	6	-	-	-	0.7	0.37
1-21-15	3	1.411	A	6	-	-	-	1.75	0.427
1-21-16	3	1.608	A	6	-	-	-	1.333	0.393
10-4-8	3	1.180	A	9	-	-	-	0.91	0.27
10-4-9	3	1.278	A	9	-	-	-	1.1	0.043
1-21-17	3	1.443	A	9	-	-	-	1	0.294
1-21-18	3	1.617	A	9	-	-	-	1.85	0.343
10-4-11	3	1.135	C	4	-	-	-	0.3	0.81
10-4-12	3	1.220	C	4	-	-	-	1.4	0.8
1-30-23	3	1.399	C	4	-	-	-	1.4	0.79
1-30-24	3	1.517	C	4	-	-	-	1.3	0.703
10-4-14	3	1.144	C	6	-	-	-	0.4	0.74
10-4-15	3	1.245	C	6	-	-	-	0.7	0.61
1-30-21	3	1.355	C	6	-	-	-	1.1	0.67
1-30-22	3	1.493	C	6	-	-	-	1.27	0.557
10-4-17	3	1.149	C	9	-	-	-	1	0.24
10-4-18	3	1.231	C	9	-	-	-	0.9	0.41
1-30-19	3	1.378	C	9	-	-	-	0.91	0.323
1-30-20	3	1.490	C	9	-	-	-	1.6	0.363
10-22-1	1	1.203	C	4	-	-	-	-	0.67

DATE/R	C	U/UM	D	H	FE4	FE6	FE8	FEMER	%VOID
10-22-2	1	1.391	C	4	-	-	-	-	0.67
10-22-3	1	1.531	C	4	-	-	-	-	0.64
10-22-4	1	1.197	C	6	-	-	-	-	0.4
10-22-5	1	1.393	C	6	-	-	-	-	0.48
10-22-6	1	1.664	C	6	-	-	-	-	0.56
10-22-7	1	1.270	C	9	-	-	-	-	0.29
10-22-8	1	1.412	C	9	-	-	-	-	0.39
10-22-9	1	1.669	C	9	-	-	-	-	0.48